Available online at www.sciencedirect.com
SCIENCE DIRECT
Polymer 47 (2006) 961–971
polymer
www.elsevier.com/locate/polymer

# Electrically conductive hydrogel composites made of polyaniline nanoparticles and poly(*N*-vinyl-2-pyrrolidone)

C. Dispenza [a,b,*], C. Lo Presti [a], C. Belfiore [a], G. Spadaro [a,b], S. Piazza [a]

[a] *Dipartimento di Ingegneria Chimica dei Processi e dei Materiali, Università degli Studi di Palermo, Viale delle Scienze, 90128 Palermo, Italy*
[b] *Centro Interdipartimentale di Ricerca sui Materiali Compositi (CIRMAC), Università degli Studi di Palermo, Viale delle Scienze, 90128 Palermo, Italy*

Received 12 July 2005; received in revised form 16 December 2005; accepted 20 December 2005

**Abstract**

A novel electrically conductive composite material, consisting of polyaniline (PANI) nanoparticles dispersed in a polyvinyl pyrrolidone (PVP) hydrogel, was prepared 'in situ' by water dispersion polymerisation (DP) of aniline using PVP as steric stabiliser, followed by γ-irradiation induced crosslinking of the PVP component. Conversion yield of aniline into PANI particles was determined via HPLC and gas chromatography, while structural confirmation of the synthesised polymer was sought by FTIR. Morphology and dimensions of PANI particles into the coloured, optically transparent hydrogel was determined by electronic microscopy; moreover, swelling behaviour of composite hydrogels in different buffer solutions was investigated by gravimetric measurements and compared to that of pure PVP hydrogels.

Cyclic voltammetry experiments were carried out both on these hydrogels and on the parent aqueous dispersions, at different pH values of the suspending/swelling medium, while conductivity of the composite hydrogels was derived from Impedance Spectroscopy; in both cases results were compared to those relative to hydrogels containing commercial-grade PANI particles.


*Keywords:* Polyaniline; Hydrogel composites; Conductivity

## 1. Introduction

Electrically conducting polymers (ECPs), and in particular polyaniline, polypyrrole, polythiophene and their derivatives, are subject of intensive research for their unique electrical, electrochemical and/or optical properties. These materials are finding growing applications in a number of industrial sectors, including optoelectronics and microelectronics (as FET, MISFET and LED [1,2]) bioelectronics (e.g. for biosensors or individual cells manipulation [3,4]), paints and coatings (as charge dissipative coatings, corrosion resistant coatings, electromagnetic shielding [5–8]), etc.

ECPs are also named 'conjugated polymers' because they are macromolecules containing a spatially extended π-bonding system, which is the reason of their intrinsic semiconducting nature. Generally, conjugated polymers become electrically conductive by means of doping reactions (e.g. using bromine and iodine vapours, as reported for polyacetylene, or by acid-base reactions with protonic acids [9]).

Polyaniline (PANI) is one of the most promising conducting polymers due to a good combination of properties, stability, price and ease of synthesis. It exists in a variety of reversible protonation and oxidation forms, differing for electrical, electrochemical and/or optical properties: the most reduced form, commonly named leucoemeraldine, consists of phenylene rings joined together by amine-type nitrogens. The fully oxidized polyaniline (pernigraniline) presents phenylene and quinoid rings in 1:1 ratio, separated by imine nitrogens. The half oxidized form (emeraldine) has imine and amine atoms of nitrogen in equal numbers, but the ratio of phenylene to quinoid rings is 3:1 [10].

The electrical conductivity ($\sigma$) of these different forms can range between $10^{-1}$ and 1 S/cm, for the most conductive protonated emeraldine, and $10^{-8}$–$10^{-10}$ S/cm, for the emeraldine base form, whereas pernigraniline base and leucoemeraldine are both non-conductive [11]. However, for these last, electrical conductivity can be improved by several orders of magnitude owing to some specific interactions of polymer chains, either with molecules of solvents used in preparative procedures or with moisture [12]. The different forms of PANI present also different interactions with the electromagnetic

* Corresponding author. Address: Dipartimento di Ingegneria Chimica dei Processi e dei Materiali, Università degli Studi di Palermo, Viale delle Scienze, 90128 Palermo, Italy. Tel.: +39 91 6567210; fax: +39 91 6567280.
*E-mail address:* dispenza@dicpm.unipa.it (C. Dispenza).

0032-3861/$ - see front matter © 2006 Elsevier Ltd. All rights reserved.
doi:10.1016/j.polymer.2005.12.071

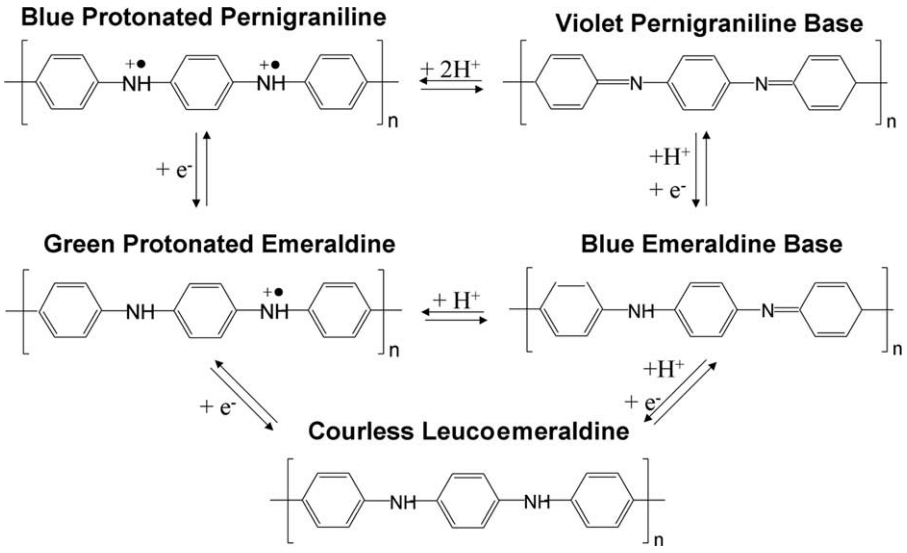


Scheme 1.

radiation in the UV–vis range, showing characteristic absorbance spectra and, thus, colours. Leucoemeraldine is colourless, protonated emeraldine is green, its corresponding half-oxidized base form is blue, whilst pernigraniline base is violet. Scheme 1 shows the different forms of PANI and their transformations by either acid/base or electrochemical reactions [13].

Like many ECPs, PANI is difficult to process because it is soluble only in a limited number of organic solvents [14], due to its highly aromatic nature and to the intermolecular hydrogen bonding between amine groups (donors) and imine groups (acceptors) of adjacent chains. On the other hand, many applications require casting the polymers as thin films or thin coatings; therefore, processability is a key issue. Further to that, exploiting reversible changes in PANI properties due to pH-induced doping reactions requires an easy access of dopant molecules to polymer chains, and thus the use of polymer solutions or dispersions. Over the last decade different synthetic routes have been developed to address the problems related with processability by introducing hydrophilic substituents (such as sulfonic acid groups directly into the PANI [15]), by copolymerisation of aniline with other monomers resulting in the formation of soluble copolymers [16], by complexation of PANI with polymeric anion dopants [6,17–19], or by emulsion polymerisation [20–23], interfacial polymerisation [24] or dispersion polymerisation [25,26]. In particular, preparation of colloidal dispersions of conducting polymers is an attractive approach, as it enables film casting from aqueous or non-aqueous solutions, either as stand-alone conducting polymers or as composite materials with other polymers [27–29]. Of course, care must be taken that the unique inherent properties of PANI are retained in its colloidal state as well, even considering that properties of polymer colloids are strongly dependent on their morphological structure. Therefore, it is required that structure of colloidal particles can be controlled.

The above-mentioned preparation methods belong the category of ‘synthetic methods’, based on aniline polymerisation in the presence of a matrix polymer or inside it; main advantages of these methods are the relative low cost of aniline as starting material and the uniformity of the PANI particles distribution into the host polymer. Another possible approach is ‘physical blending’, which can be either solution blending of substituted/doped soluble PANI or dry blending of PANI with another polymer followed by melt processing. Physical blending has been reviewed recently by Pud et al. [30], who have also highlighted the serious difficulty, related to the great variety of preparative methods of PANI blends or composites, of rationalising differences in the properties of materials prepared under seemingly similar conditions. In fact, the response of these materials seems to be governed by the specific physicochemical interactions among the different components (PANI–dopant, PANI–host polymer, dopant–host polymer), which in turn depend on method and conditions of material formation, on the quantitative ratios between material components, on raw materials properties, etc.

In our approach, doped PANI particles were first synthesised from aniline, following a conventional aqueous dispersion technique [26], using poly(*N*-vinyl-2-pyrrolidone) (PVP) acting both as a site for adsorption of oligoaniline initiation centres and as steric stabiliser of the formed colloidal PANI particles [31]. Then, this colloid was transformed into a soft and wet hydrogel/PANI composite, whose matrix material is the same PVP formerly used as steric stabiliser and that, after PANI synthesis, was chemically crosslinked by means of $\gamma$-irradiation. Alternatively, a commercial PANI was dispersed in water, always in the presence of PVP, and then crosslinked via $\gamma$-irradiation, similarly to the ‘in situ’ synthesised PANI. Aim of this investigation is to prepare highly conductive hydrogel composites of PANI nanoparticles that shall allow reversible doping/undoping reactions in the swollen state and the related changes of conductivity and optical properties. Hydrogels capable of reacting to environmental stimuli like pH, electric field and light, can be designed for use in the so-called ‘intelligent biomaterials’, whose application is a driving

innovation in medicine and pharmacy [3,4]. The inherent flexibility of PVP hydrogel should also allow the formation of supramolecular structures in the dry state due to self-assembly of PANI particles, as already reported for PANI–HCl/PVA blend films [32]. Chemical crosslinking among PVP chains should improve chemical stability of the composite both in the swollen and in the dry state. Structural, morphological, and electrical properties of both the 'in situ' synthesised PANI/PVP and the 'dispersed' PANI/PVP hydrogel composites are discussed below.

## 2. Experimental

Poly(*N*-vinyl-2-pyrrolidone) (PVP K60, with $M_w$ = 160,000, supplied as 45 wt% aqueous solution by Fluka), aniline (purity: 99.5%), ammonium persulfate (purity: 99.99%), hydrochloric acid (37 wt%) and a commercial grade polyaniline (in the form of emeraldine base, with $M_w$ = 5000), all supplied by Aldrich, were employed as received.

For the synthesis of PANI, an aqueous solution of PVP was prepared at room temperature by dissolving 4 g of PVP in 100 ml of deionised water; 5 ml of HCl were then added to the above solution. The resulting system was deoxygenated under a constant flow of nitrogen and then 1 g of aniline was added. The redox initiator aqueous solution was prepared separately, by dissolving 5.3 g of ammonium persulfate in 50 ml of deionised water. Both solutions were cooled down to 4 °C and mixed in order to start polymerisation; during reaction the mixture was stirred and always maintained at 0–4 °C, under nitrogen atmosphere. Reaction was carried out for 24 h: during synthesis the reaction mixture, initially colourless, immediately turned blue and later green, according to the formation of protonated emeraldine [26]. Both HPLC and GC analysis, carried out on small samples withdrawn from the reactor at regular intervals, proved that after the first 30 min the aniline was no longer present in the reaction mixture.

Being synthesised in highly acidic conditions, polyaniline was produced in its doped state in the form of protonated emeraldine (PANI–PE) at pH = 1.6 and converted into pernigraniline by adjusting the pH value to 9 by addition of concentrated aqueous sodium hydroxide. Dispersions were green at pH = 1.6 and violet at pH = 9.

After synthesis, dispersions were sealed and stored at 4 °C; before irradiation they were diluted tenfold using the PVP solution (4 wt%/vol), so that PVP concentration was kept constant. PANI/PVP hydrogel composites were obtained by $^{60}$Co γ-irradiation of the diluted dispersions of synthesized PANI. Irradiation was performed in glass vials under nitrogen at a dose rate of 2 kGy/h and a total absorbed dose of 40 kGy. During irradiation, temperature was maintained at 10 °C. Synthetic PANI/PVP hydrogel composites were produced at the two pHs of 1.6 and 9: they were both transparent and green and violet in colour, respectively.

Hydrogels were also produced in the same conditions as above, starting either from aqueous solutions of PVP only or dispersions of commercial PANI in the presence of PVP. These last were obtained by vigorous stirring of the 4 wt%/vol aqueous PVP/water solution containing 0.06 wt% PANI powder. Dispersions of commercial PANI proved to be less stable than previous ones upon storage; therefore, they were always stirred before γ-irradiation. In both cases the pH of hydrogels was 5.8. The pure PVP hydrogel is colourless and transparent, whilst the commercial PANI/PVP hydrogel composite is transparent blue.

FTIR analysis was performed in the 4000–400 $cm^{-1}$ range using a Perkin–Elmer spectrophotometer. Measurements were carried out in the transmission mode on commercial PANI–EB and freeze dried powders of PVP, PVP hydrogel, synthetic PANI/PVP dispersion and synthetic PANI/hydrogel composite; samples were prepared in form of KBr tablets. Spectra of synthetic PANI/PVP dispersions and synthetic PANI/hydrogel composites were normalised to the absorbance at 1653 $cm^{-1}$, referring to the carbonyl stretching band of PVP.

Swelling behaviour of composite hydrogels was investigated by gravimetric measurements and compared to that of pure PVP hydrogels. After removing the excess surface liquid by centrifugation for 2 min at 2000 rpm, the initial swelling ratio of the hydrogels (ISR: ratio between the initial weight of the hydrogel and the corresponding freeze–dried sample) was determined. Freeze–dried hydrogels were re-hydrated into different buffer solutions at a constant temperature of 5 °C and the re-hydration ratio (RR) was calculated as the ratio between the weight of re-hydrated hydrogel and the corresponding initial freeze–dried sample. Buffer solutions at three different pHs (4.5, 7.4 and 10) and almost constant ionic strength (0.20–0.25 mol/l) were used. Samples were withdrawn and weighed at regular intervals (every hour) during day time and left immersed overnight (for maximum 10 h). Reported results are averaged over five measurements and the standard deviations were always below 8%.

In order to get a first insight on dimension and morphology of PANI particles for both the 'in situ' synthetised PANI/PVP dispersion and the physically dispersed PANI/PVP system, SEM analysis was performed, by means of a Philips scanning electron microscope (ESEM, XL-30), onto thin films obtained according to the following procedure: dispersions were diluted up to 500 times with distilled water, dropped onto aluminium supports and air-dried at room temperature. Morphology of the hydrogels after freeze–drying was also investigated: in all cases samples were gold sputtered prior to SEM analysis, in order to enhance contrast.

Investigation of the electrical properties was performed both by cyclic voltammetry (CV) and impedance spectroscopy (IS). CV experiments were carried out, both on the hydrogel and on aqueous dispersions of synthetic and commercial PANI at different pHs, in a three-electrode cell having Pt as working and counter electrodes and a saturated calomel (SCE) as reference electrode, in connection with the cell through a Luggin capillary. For CV experiments a potentiostat/function generator (AMEL, SYSTEM 5000) coupled to an oscilloscope (NICOLET) was employed, and data were acquired by a desk computer. IS analysis was performed on hydrogels in

a two-electrode cell at room temperature by means of a frequency response analyser (FRA, Schlumberger, mod.1255), applying an AC signal with 0.1 V peak-to-peak and 0.5 V bias. The analyser was connected with a dielectric interface (Chelsea), in order to measure up to very high impedances. The measuring unit consisted of two circular gold electrodes (diameter: 10 mm) with a MACOR ring separator (height: 2 mm). The capacitance of the separator was 1.1 pF, thus giving a parallel impedance much higher than the measured ones in the investigated frequency range ($10^{-2}$–$10^{5}$ Hz). For shielding electromagnetic interference, measuring cell and apparatus were placed in a Faraday cage; data were acquired by a desk computer and processed according to the ZVIEW 2™ software.

## 3. Results and discussion

### 3.1. Structural characterization

FTIR analysis was performed on samples of commercial PANI–EB, before and after γ-irradiation at 40 kGy in the solid state. The spectrum of irradiated commercial PANI–EB and that of the not irradiated polyaniline match exactly (Fig. 1, curve a). In this spectrum the prominent absorption peaks at 1590 and 1494 $cm^{-1}$ are attributed to the quinoid and phenylene ring deformation, respectively, the relative intensity of these bands giving an indication of the oxidation state of EB [33,34]. The bands 1301 $cm^{-1}$ and in the 1237–1210 $cm^{-1}$ range can be assigned to $C_{ar}$–N stretching and C–N, and respectively [34]; peaks at 1378 and 1163 $cm^{-1}$ correspond to C–C stretching of quinoid and C–H in plane bending of phenylene; finally, the band at 828 $cm^{-1}$ is from the C–H out-of-plane bending mode of quinoid units [33].

FTIR spectrum of PANI–PE/PVP dispersion (Fig. 1, curve b) shows the characteristic absorption peak of PANI at 1505 $cm^{-1}$, while the peak at higher wavenumber is no longer evident as all quinoid units are converted in phenylene units in the HCl doped emeraldine. The absorptions at 1653 $cm^{-1}$ and in the 3020–2830 $cm^{-1}$ range are attributed to PVP and, in particular, are related to the absorption of the carbonyl present in the >C(=O)–N– group and to the symmetrical and asymmetrical stretching of C–H in $–CH_2–$. The peak at 1653 $cm^{-1}$ is considerably shifted with respect to the expected free carbonyl group absorption at 1680 $cm^{-1}$, due to interactions with PANI macromolecules via intermolecular H-bonding [35,36]. Distinctive features of PANI–PE in the dispersions are the absorption at 3120, 1200 and 1138 $cm^{-1}$: peaks at 3210 and 1138 $cm^{-1}$ are related to vibration modes of $N–H^{+}–$ and/or $–NH^{+}=$, present into the doped PANI backbone but, possibly also formed by protonation of the imides groups of PVP at low pH; the peak at about 1200 $cm^{-1}$ is interpreted as originating from the bipolaron structure, related to C–N stretching vibration [35].

Finally, the sharp peak at about 1400 $cm^{-1}$, corresponding to N–H valence frequency and N–H deformation, can be interpreted as a result of the strong H-bonding of N–H with >C=O groups of PVP [35].

In Fig. 2 FTIR spectra of PVP (not irradiated), PVP hydrogel and synthetic PANI/PVP hydrogel composite are shown. The spectrum of PVP (curve a) presents the already discussed bands at 3020–2830 and 1653 $cm^{-1}$ and also relevant absorptions at 3690–3060 and 2250–1900 $cm^{-1}$. The shifted position of the carbonyl absorption [37] and the bands in the 3690–3060 and 2250–1900 $cm^{-1}$ regions can be related to the presence of 'bound' water, not eliminated by the freeze–drying process. The content of 'bound' water appears to be reduced in PVP hydrogels (curve b), probably due to mobility restraints induced by crosslinking: in fact the absorptions related to 'bound' water are reduced in intensity and structuring. It can also be observed that the carbonyl absorption is positioned around the most conventional wavenumber of 1680 $cm^{-1}$. The FTIR spectrum of synthetic PANI/hydrogel composite (Fig. 2, curve c) closely resembles the spectrum of PVP hydrogel, as expected considering that the amount of PANI in the composite is very low (0.6 wt% in dry samples). The presence of interactions among the phases is

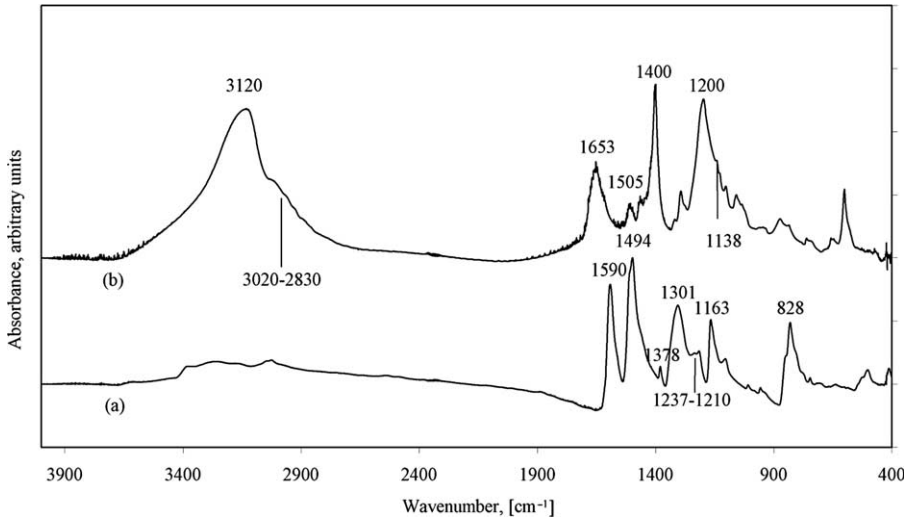


Fig. 1. FTIR analysis of (a) irradiated commercial PANI, (b) PANI-PE/PVP dispersion.

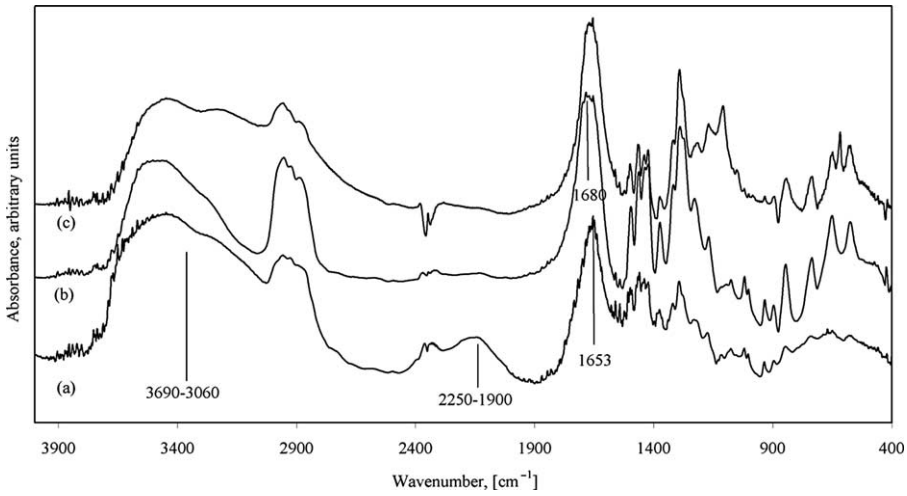


Fig. 2. FTIR analysis of (a) not irradiated PVP, (b) PVP hydrogel, (c) synthetic PANI /hydrogel composite.

witnessed by the wide and structured absorption in the 3700–3000 cm$^{-1}$ region and by the shift of the characteristic carbonyl absorption towards lower wavenumbers.

### 3.2. Morphological characterization

Morphological analysis has been performed on: (1) air dried dispersions at different dilution levels; (2) freeze–dried hydrogels. The SEM image (Fig. 3) of an air-dried film obtained from the original (more concentrated) synthetic PANI dispersion at pH = 1.4 reveals, for the synthetic PANI/PVP system only, a dendritic structure, at variance with the corresponding system obtained from the commercial PANI dispersion, showing a globular structure.

In the attempt to resolve morphology of single PANI particles SEM analysis has been carried out also on solid deposits from highly diluted (with pure water) dispersions; in fact at high dilution levels particles agglomeration, as a result of the drying process, should be minimized and the single PANI particles with their PVP-rich shell resolved. Figs. 4 and 5 show SEM images of dried-down polyaniline particles. It can be observed that the morphological structure of polyaniline prepared by either physical blending polymeric emeraldine base with PVP (Fig. 4) or by 'in situ' reacting aniline in the presence of PVP to give polymeric protonated emeraldine (Fig. 5) are both globular. Fig. 4 shows agglomerates of 80 nm average diameter globular particles, whereas Fig. 5 presents spherical particles with an average diameter of 30 nm on the background and bigger agglomerates on the foreground.

SEM image of the freeze–dried hydrogel containing synthetic PANI evidences a tendency of PANI particles to organise into needle-like structures (Fig. 6).

### 3.3. Swelling behavior

In order to determine the amount of water incorporated in the network structure formed by γ-irradiation the initial swelling ratio of the hydrogels has been measured; results are reported in Table 1. All the hydrogel composites present an initial water content lower than that of the hydrogel made with PVP only, and the ISR values for the composite hydrogel are very little influenced by pH. In all cases water is by large the main component of these systems, but the PVP network ability to deform, absorbing large quantities of water, is affected by the presence of the more rigid and less hydrophilic PANI polymer in the composite hydrogel.

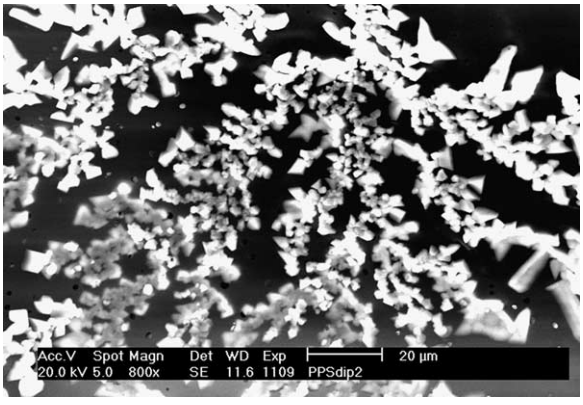


Fig. 3. Electron microscopy of the air-dried film obtained from the original synthetic PANI dispersion.

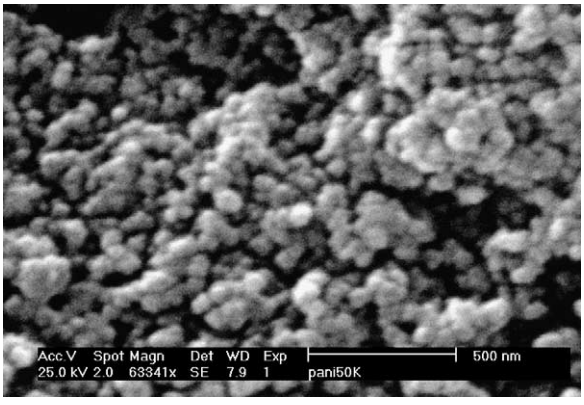


Fig. 4. Electron microscopy of the air-dried film obtained from highly diluted commercial PANI dispersion.

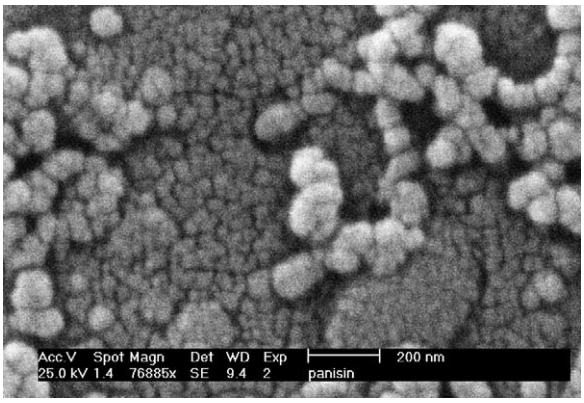


Fig. 5. Electron microscopy of the air-dried film obtained from highly diluted synthetic PANI dispersion.

The rehydration capability of the PVP and synthetic PANI/PVP hydrogels from the dry state is depicted in Fig. 7: curves relative to the pure PVP hydrogel lie below curves referring to the composite irrespective of pH; after the first hours of immersion the RR values for the composite hydrogel are very similar to the corresponding ISR values (around 24); on the contrary RR values for PVP hydrogels are significantly lower than ISR. Therefore, it appears that the presence of PANI hinders the interactions among macromolecular segments of PVP, that are prevalently exerted in the shrunk state of the dry hydrogel and not completely reversed by the presence of solvent molecules in the swollen state.

Quite interestingly, the semi-interpenetrating network structure of the PANI/PVP hydrogel allows reversible shrinking/swelling processes, as also proved by repeated rehydration/dehydration cycles performed with the system at pH = 1.6. This property can have a tremendous impact on the development of 'intelligent' biomaterials.

### 3.4. Cyclic voltammetry

In order to test system stability, CV experiments have been carried out on the different hydrogels in an aerated glass three-electrode cell (Section 2); moreover, for checking the electroactive behaviour of polymer particles, the parent aqueous

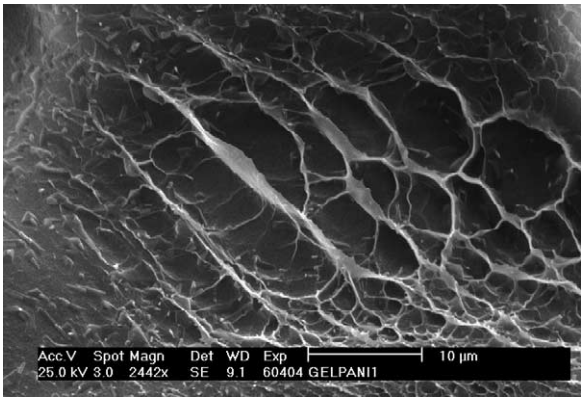


Fig. 6. Electron microscopy of the freeze–dried hydrogel containing synthetic PANI.

Table 1
Initial swelling ratio of the PVP hydrogel and the different composite hydrogels

| Hydrogel composition | pH | ISR |
|---|---|---|
| PVP | 5.8 | 38 |
| Commercial PANI/PVP | 5.8 | 24 |
| Synthetic PANI/PVP | 1.6 | 23 |
| Synthetic PANI/PVP | 9 | 21 |

dispersions containing PANI particles have been also investigated before γ-irradiation. In this last case CV investigation has been performed both in contact with air and under nitrogen atmosphere. In this paper we will report results pertaining to the following samples:

1. Hydrogel containing commercial PANI–EB at pH = 5.8.
2. Hydrogel containing synthetic PANI–PE at pH = 1.6.
3. Dispersions containing synthetic or commercial PANI at different pHs.

The hydrogel containing commercial PANI–EB particles shows a large stability interval (between +1.05 and −0.85 V/SCE, approximately) delimited by the water decomposition reactions. Beyond this interval oxygen and hydrogen evolution take place, with visible bubbling on the electrodes, in the anodic and cathodic polarization regions, respectively. No oxidation/reduction peak is observed within the stability interval, with the exception of a small cathodic peak in the reverse scan after that electrode potential is increased up to over +0.9 V/SCE. However, when the upper potential limit is lower then +0.9 V, this cathodic peak disappeared, being thus associated to some oxidation product formed in the region of oxygen evolution.

The hydrogel containing synthetic PANI–PE at pH = 1.6 shows a slightly narrower stability interval, especially in the negative potential region where hydrogen evolution takes place at about −0.4 V/SCE, but in this case an anodic oxidation wave is present in the forward scan of the voltammogram at about +525 mV/SCE; no reduction peak was observed in the reverse scan. We mention that the anodic peak potential ($E_{pa}$) is practically independent of scan limits and that its current intensity ($I_{pa}$) is increasing almost linearly with the square root of the sweep rate (50–200 mV/s). This last feature is typical of both kinetically reversible or fully irreversible processes [38]; however, the investigated rate interval is too low in order to reach final conclusions on this point.

The absence of a cathodic peak in the reverse scan could be ascribed to a very low mobility of the oxidation product or to its fast depletion owing to a homogeneous chemical reaction. For comparison we have performed experiments on aqueous dispersions of PANI particles with different pH values. Within the stability interval, no oxidation/reduction peaks were observed in the voltammograms relative to dispersion containing commercial PANI particles, both at pH = 1 and 6.8, nor in dispersion of synthetic PANI particles at pH = 9. On the contrary CV experiments carried out in aqueous dispersion of synthetic PANI at pH = 1.4 displays both an anodic peak, at about 535 mV/SCE, and a cathodic peak, at about 80 mV/SCE.

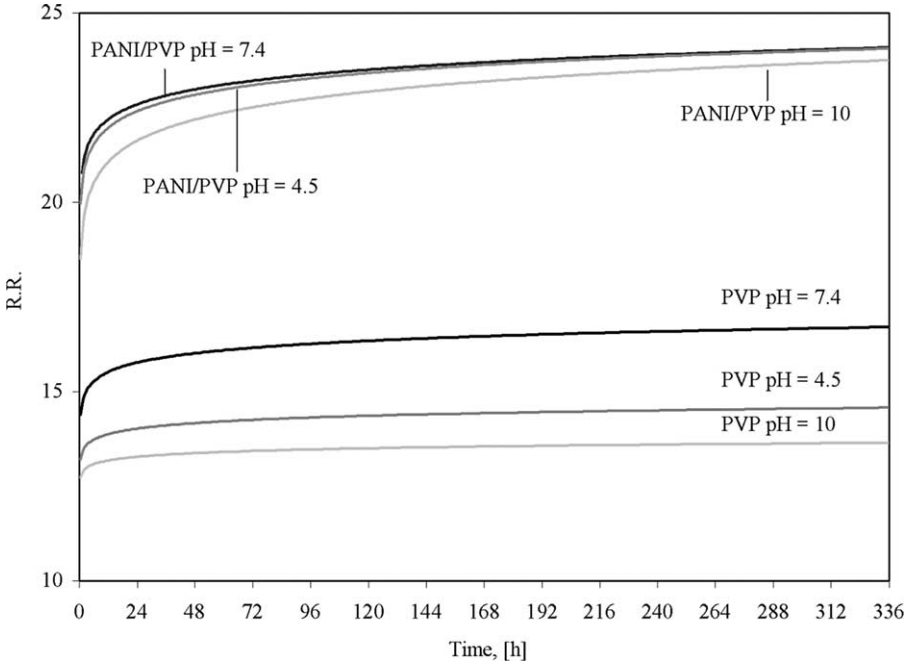


Fig. 7. Re-hydration ratios as a function of immersion time at three different pH for PVP hydrogel and synthetic PANI/ PVP hydrogel composite.

Again no influence of scan limits has been observed on peak potentials.

This measurement has been also performed under nitrogen atmosphere, and the results are reported in Fig. 8: in this case, we observe an anodic peak at about 560 mV/SCE and a cathodic peak at about 55 mV/SCE, with a ratio between anodic and cathodic peak current ($I_{pa}/I_{pc}$) very close to unity, whilst for experiments performed in air, $I_{pa}/I_{pc}$ values sensibly lower than 1 should be ascribed to the contribution of oxygen reduction to the measured cathodic current.

Table 2 summarizes results obtained in different environments and reports peak potentials.

The voltammetric behaviour of polyaniline has been widely investigated in the literature. A detailed study [39] has shown that cyclic voltammograms of chemical synthesized and electrochemically deposited PANI are identical; in acidic (HCl) solutions they present two oxidation peaks at around 0.15 V/SCE and at 0.2–0.8 V/SCE, respectively. This second peak shifts of about 120 mV per pH unit, whilst the first one shows a pH dependence (58 mV per pH unit) only below pH = 0, being constant at higher pH values. Similar dependences were observed for the corresponding reduction peaks in the return scan. All these findings are confirmed by others [40]; moreover, very similar features characterize CV curves recorded also for crystalline aniline oligomers and thin PANI films grown onto metal electrodes [41,42]: in all cases two well separated oxidation/reduction waves are recorded within the water stability potential interval. It is widely accepted [39] that the first oxidation/reduction wave, at lower potential, can be attributed to the equilibrium between the leucoemeraldine form of PANI (insulator) and protonated emeraldine form of PANI, which presents a metallic conductivity (see also below). Such equilibrium involves no protonation/deprotonation, at variance with the second oxidation peak attributed to the oxidative deprotonation of protonated emeraldine to give pernigraniline base (insulator), with a ratio of two protons per electron involved.

By comparing our results with literature data, we can assign the oxidation peak recorded at 525–560 mV/SCE for both the acidic dispersion and the hydrogel containing synthetic PANI to

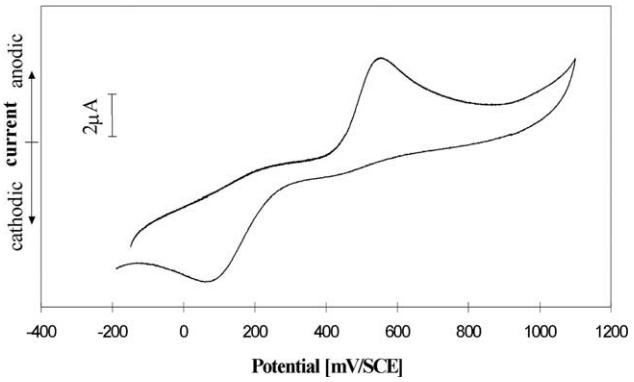


Fig. 8. CV of acidic synthetic PANI dispersion under $N_2$.

Table 2
Anodic and cathodic peak potentials for different dispersions/hydrogels containing PANI particles

| Sample | pH | Atmosphere | $E_{pa}$ (mV/SCE) | $E_{pc}$ (mV/SCE) |
|---|---|---|---|---|
| Disp. of comm. PANI | 6.8 | Air | No peak | No peak |
| Disp. of comm. PANI | 1 | Air | No peak | No peak |
| Hydr. of comm. PANI | 5.8 | Air | No peak | No peak |
| Disp. of synt. PANI | 9 | Air | No peak | No peak |
| Disp. of synt. PANI | 9 | Nitrogen | No peak | No peak |
| Disp. of synt. PANI | 1.4 | Air | 535 | 80 |
| Disp. of synt. PANI | 1.4 | Nitrogen | 560 | 55 |
| Hydr. of synt. PANI | 1.6 | Air | 525 | No peak |

the oxidative deprotonation of protonated emeraldine; according to data reported in [39], such oxidation should have a half-peak potential of about 550 mV/SCE at pH around 1.5, in excellent agreement with our data. This means that reactivity of PANI nanoparticles, both in stabilized aqueous dispersions and in the hydrogel, is the same as that of thin PANI films. We mention also that recently an almost coincident oxidation peak has been reported in CV of dispersions of polyaniline colloids in 1.25 M HCl [27]. The absence of such oxidation peak in neutral or slightly alkaline systems is expected, because at these pH values protonated conductive emeraldine does not form, as testified by the different colours of the hydrogel/dispersions. The absence of the corresponding reduction peak in the reverse scan suggests that at pH = 1.6 pernigraniline, formed at the electrode surface, is quickly chemically protonated. Thus, CV analysis confirms a stabilization of the protonated form of PANI in strongly acidic environments.

The absence of the first oxidation wave, at lower potential, must be ascribed to the fact that our starting systems consist already of protonated emeraldine, whilst in the return scan voltammograms show a reduction peak at 55–80 mV/SCE only for the dispersions, due to the above mentioned stabilization of protonated emeraldine (maybe stronger in the hydrogel than in the dispersion): in fact this reduction peak is attributable to the surface reduction of emeraldine in contact with the Pt electrode to leucoemeraldine. No change of bulk colour could be observed, involving this reaction only a small part of the dispersion.

Interestingly, the voltammetric behaviour of PANI is related to its conductivity. At acidic pH values conductivity of PANI thin films shows a broad maximum (up to 5 S/cm) in the potential interval between the two oxidation peaks in the voltammogram, and falls down of several orders of magnitude at potentials more anodic than the second peak or more cathodic respect to the first oxidation peak [41,43]. The conductivity changes are reversible, provided that the potential is kept below the oxygen evolution region [41,44]. Finally, thermopower experiments at room temperature evidence the strong influence of pH on PANI conductivity, with a maximum at around pH = 1 and a sharp metal–insulator transition above pH = 3 [45]. All these studies reveal an unique electrical characteristic of PANI, whose conduction depends on both pH and oxidation state [11,41], and suggest that its metallic conductivity is due to the very high doping levels attainable, which cause the gap states to broaden into a continuous half-filled band [45].

### 3.5. Impedance spectroscopy

In order to test conduction of our hydrogels, the frequency dispersion of system impedance has been measured at room temperature in a two-electrode cell filled with the hydrogel containing commercial PANI–EB at pH = 5.8, with the hydrogels containing synthetic PANI both at pH = 1.6 and 9, or, for comparison, with the hydrogel containing PVP only. As shown in Fig. 9, Nyquist diagrams are usually distorted

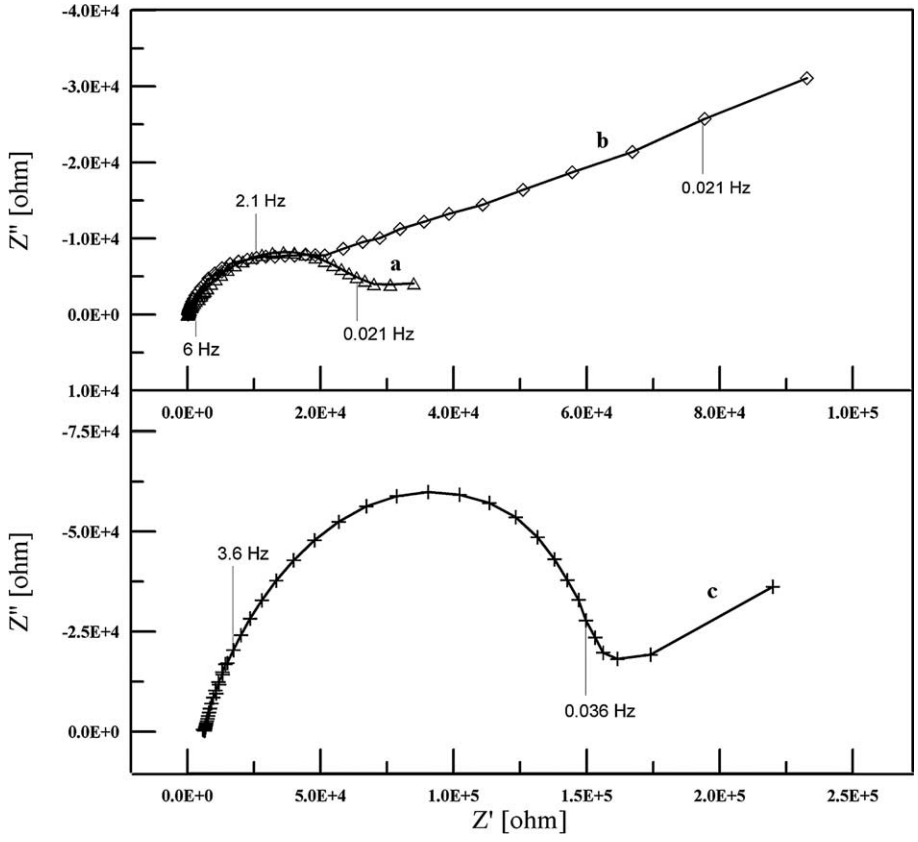


Fig. 9. Nyquist plots of hydrogels with: (a) synthetic PANI at pH = 1.6, (b) synthetic PANI at pH = 9.1, (c) commercial PANI.

semicircles, sensibly smaller in the case of hydrogels containing synthetic PANI–PE (curve a), followed by a small linear zone in the low frequency region, suggesting the presence of mass transport phenomena within the composite hydrogel; only for the hydrogel containing synthetic PANI at pH = 9 the semicircle is largely incomplete and the linear region much more expanded (Fig. 9, curve b). The Nyquist diagram relative to the hydrogel containing commercial PANI (Fig. 9, curve c) reveals more resistive behaviour (higher diameter of the semicircle) with respect to the system containing synthetic PANI. In the Bode diagrams negative impedance phase angle with a sharp minimum is evidenced in all cases: frequency at which minimum phase angle occurs is lower for hydrogels without PANI or containing commercial PANI (between 3 and 10 Hz, approximately) than for hydrogels containing synthetic PANI (about 100 and 700 Hz, at pH = 9.1 and 1.6, respectively). Moreover, the minimum peak in phase angle is broader in the case of the hydrogel containing synthetic PANI–PE at pH = 1.6.

Fitting of the previous data according to different electrical equivalent circuits gave no satisfying results, despite their relatively simple shape. In analysing impedance data we, therefore, have adopted the formalisms of complex impedance, $Z^*$, and permittivity, $\varepsilon^*$ [46], in order to describe dielectric relaxation phenomena and to determine the bulk conductivity of our hydrogels; the latter should reflect also ionic mobilities in the water–swollen gel [47].

This approach was shown very powerful for interpreting dielectric relaxation spectroscopy (frequency range: 5 Hz to 2 GHz) on poly(hydroxyl-ethyl-aspartamide) (PHEA) hydrogels with varying water content and at different temperatures [48]. According to this approach, the complex dielectric function can be calculated as:

$$\varepsilon^*(\omega) = \frac{Y^*(\omega)}{i\omega C_0} = \frac{C}{C_0} - i\frac{G}{\omega C_0} = \varepsilon'(\omega) - i\varepsilon''(\omega) \quad (1)$$

where $Y^* = [Z^*(\omega)]^{-1}$ is the measured complex admittance, $C$ and $G$ the measured capacitance and conductance, $\omega$ the angular frequency ($\omega = 2\pi f$) and $C_0$ the equivalent capacitance of the free space. The frequency-dependent AC conductivity, $\sigma'(\omega)$, is then obtained as [46]:

$$\sigma'(\omega) = \varepsilon''(\omega)\omega\varepsilon_0 \quad (2)$$

where $\varepsilon_0$ is the permittivity of free space and $\varepsilon''$ the imaginary part of complex permittivity.

Fig. 10 shows the $\sigma'(\omega)$ vs. frequency diagram for the different samples under 0.5 V bias: by taking into account the different frequency interval investigated with respect to Ref. [48], the much higher water content of our hydrogels and the higher temperature, we can assume that the plateau at intermediate to high frequencies corresponds to the DC conductivity, $\sigma_{dc}$, of the hydrogels. The decrease of $\sigma'(\omega)$ at low frequencies could reflect both electrode polarization and the presence of diffusion phenomena (see the Nyquist plots of Fig. 9), whose influence extends over frequencies not investigated in [48]; on the contrary, our experimental apparatus did not allow to investigate the transition from long-range to short-range mobility in the hydrogels, which should occur far in the MHz region or beyond. For the same reason the analysis of the complex electric modulus, $M^*$ [48,49], gave us no useful information: in fact, considering the extremely high water content in our hydrogels and the working (ambient) temperature, peaks in the $M''(\omega)$ plots are expected at much higher frequencies than those investigated. Moreover, our systems are much more conducting (4 orders of magnitude or more) with respect to the PANI chemically synthesized in [49].

Results reported in Fig. 10 can be summarized as follows.

(a) All hydrogels display remarkable conductivity, owing to their extremely high water content (about 96% by weight).
(b) Addition of commercial PANI–EB to the hydrogels results in no beneficial effect on conductivity. This fact is not unexpected, considering that emeraldine base presents an insulating behaviour.

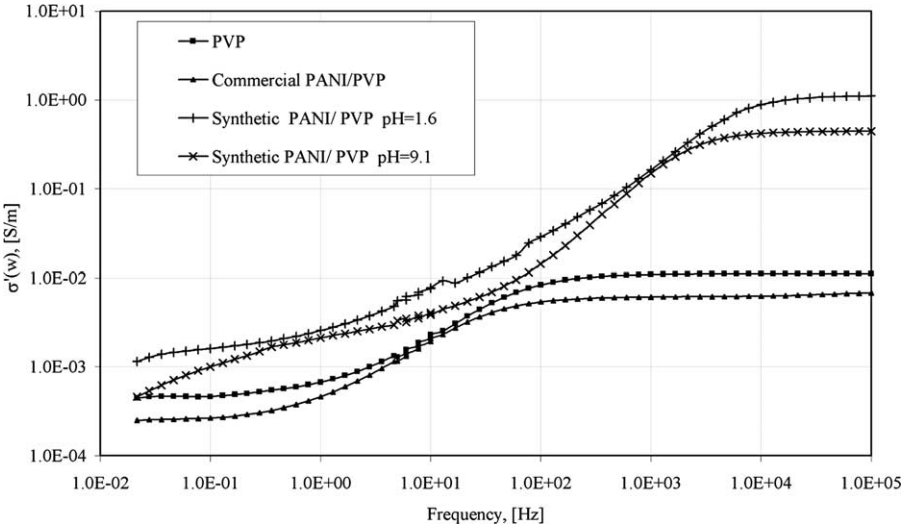


Fig. 10. Conductivity of hydrogels as a function of frequency.

(c) For hydrogels containing 'in situ' synthesised PANI DC conductivity is much higher (almost two orders of magnitude) with respect to those containing commercial polymer particles or containing only PVP (no PANI particles). Moreover, DC conductivity of hydrogels containing synthetic PANI increases of about 2.5 times at acidic pH.

We note that the value of DC conductivity for the hydrogel containing synthetic PANI–PE at pH = 1.6, roughly corresponds to that expected for a 0.04 M HCl aqueous solution, which is the initial hydrochloric acid concentration in our dispersion. Even considering that $H^+$ ions are partially depleted due to PANI particles protonation, this means that electrical conduction in our composite system is basically due to free ions in the water phase, including ammonium and sulfate ions from the decomposition of the oxidant agent. The same arguments hold for the hydrogel containing synthetic PANI at pH = 9, taking into account that neutralization process replace $H^+$ with (less mobile) $Na^+$ ions. Above conclusions about the conductivity of our composite systems are supported by detailed studies on the conductivity of colloidal polyaniline dispersions ([50] and references therein): for submicrometers size conducting PANI particles dispersed in an acidic aqueous medium with different concentrations ($<0.02$ g cm$^{-3}$), it was found that conductivity of PANI particles was always lower than that of the aqueous phase. In that work an attempt was made to estimate the contribution of PANI particles to the total conductivity by redispersing particles after precipitation, even if particles modification (e.g. partial aggregation) after this procedure could not be ruled out.

Previous finding does not rule out completely a possible contribution coming from conductive PANI–PE nanoparticles in the acidic system. In fact for polyaniline suspensions in a non-conducting liquid it has been suggested that particles become ordered in chains aligned with the electric field, with formation of 'conducting chains' [51]. In our case the very low PANI–PE content in the hydrogel (0.06% by weight) and the high ions concentration necessary in order to stabilize nanoparticles in the system would probably mask this contribution, if present. This aspect needs to be clarified by additional experimental work, performed on hydrogels with a much lower water content or on solid films obtained by deposition/exsiccation from the composite dispersions.

## 4. Conclusions

Conductive composite hydrogels, made of polyaniline nanoparticles dispersed in a PVP network, have been obtained by dispersion polymerisation in aqueous medium, followed by γ-irradiation. Conversion of aniline into PANI particles was almost quantitative in HCl environment, and FTIR spectra confirm polymerisation of the monomer.

Acidic PANI hydrogels display a green colour, typical of protonated emeraldine, whilst upon neutralization with NaOH a violet composite containing pernigraniline nanoparticles was obtained at pH = 9. Another composite hydrogel system was obtained by physical blending of commercial PANI–EB with PVP, followed by γ-irradiation: in this case hydrogel was blue in colour and its pH about 6.

SEM analysis, carried out on all dispersions and at high dilution levels, always shows spherical primary PANI nanoparticles, which upon concentration tend to form big agglomerates; in the synthetic PANI–PE hydrogel only, dendrite structures were resolved.

Swelling behavior, tested through ISR and hydration/dehydration cycles, reveals reversible shrinking/swelling processes for the PANI/PVP hydrogels, at variance with pure PVP hydrogels.

Cyclic voltammetry, carried out both on the hydrogel and the parent aqueous dispersions, reveals reactivity only for the acidic systems containing PANI–PE particles; potentials of characteristic peaks are in agreement with those reported in the literature for pure PANI films. However, the stability of the PANI-PE form is higher within the hydrogel environment.

IS analysis suggests that conductivity of composite hydrogels is due to their high water content, and mainly ascribed to ionic mobility. However, some contribution from the conductive PANI–PE could also be present.

## Acknowledgements

The financial support of the University di Palermo (60% funds) is gratefully acknowledged.

## References

[1] Kumar D, Sharma RC. Eur Polym J 1998;34(8):1053–60.
[2] Somani P, Mandale AB, Radhakrishnan S. Acta Mater 2000;48:2859–71.
[3] Brahim S, Narinesingh D, Guiseppi-Elie A. Biosens Bioelectron 2002;12:973–81.
[4] Adhikari B, Majumdar S. Prog Polym Sci 2004;29:699–766.
[5] Wan M, Li M, Li J, Liu Z. Thin Solid Films 1995;259:188–93.
[6] Jia W, Tchoudakov R, Segal E, Joseph R, Narkis M, Siegmann A. Synth Met 2003;132:269–78.
[7] Ogurtsov NA, Pud AA, Kamarchik P, Shapoval GS. Synth Met 2004;143:43–7.
[8] Paligová M, Vilčáková J, Sáha P, Kresálek V, Stejskal J, Quadrat O. Physica A 2004;335:421–9.
[9] Pron A, Rannou P. Prog Polym Sci 2002;135–90.
[10] Kang ET, Neoh KG, Tan KL. Prog Polym Sci 1998;23:277–324.
[11] Chiang C, MacDiarmid AG. Synth Met 1986;13:193–205.
[12] Matveeva ES. Synth Met 1996;79:127–39.
[13] Stejskal J, Kratochvil P, Jenkins AD. Polymer 1996;37:367–9.
[14] Cao Y, Qiu J, Smith P. Synth Met 1995;69:187–90.
[15] Wu Q, Xue Z, Qi Z, Wang F. Synth Met 2000;108:107–10.
[16] Kinlen J, Frushour BG, Ding Y, Menon V. Synth Met 1999;101:758–61.
[17] Sun L, Liu H, Clark R, Yang SC. Synth Met 1997;84:67–8.
[18] Schmidt V, Domenech SC, Soldi MS, Pinheiro EA, Soldi V. Polym Degrad Stab 2004;83:519–27.
[19] Lee YM, Nam SY, Ha SY. J Membr Sci 1999;159:41–6.
[20] Su M, Hong J. Synth Met 2001;123:497–502.
[21] Jeon BH, Kim S, Choi MH, Chung IJ. Synth Met 1999;104:95–100.
[22] Swapna P, Subrahmanya S, Sathyanarayana DN. Synth Met 2002;128:311–6.
[23] Ruckenstein E, Sun Y. Synth Met 1995;74:107–13.
[24] Gao H, Jiang T, Han B, Wang Y, Du J, Liu Z, Zhang J. Polymer 2004;45:3017–9.

[25] Wessling B. Synth Met 1998;93:143–54.
[26] Somani PR. Mater Chem Phys 2002;77:81–5.
[27] Atobe M, Chowdhury A, Fuchigami T, Nonaka T. Ultrason Sonochem 2003;10:77–80.
[28] Riede A, Stejskal J, Helmstedt M. Synth Met 2001;121:1365–6.
[29] Banerjee P, Mandal BM. Synth Met 1995;74:257–61.
[30] Pud A, Ogurtsov N, Korzhenko A, Shapoval G. Prog Polym Sci 2003;28: 1701–53.
[31] Stejskal J, Sapurina I. J Colloid Interface Sci 2004;274:489–95.
[32] Zhang Z, Wan M. Synth Met 2002;128:83–9.
[33] Boyer MI, Quillard S, Rebourt E, Louarn G, Buisson JP, Monkman A, et al. J Phys Chem B 1998;102:7382–92.
[34] Trchová M, Sapurina I, Hlavatá D, Prokěs J, Stejskal J. Synth Met 2001; 121:1117–8.
[35] Ghosh P, Siddhanta SK, Chakrabarti A. Eur Polym J 1999;35: 699–710.
[36] Murugesan R, Anitha G, Subramanian E. Mater Chem Phys 2004;85: 184–94.
[37] Muta H, Ishida K, Tamaki E, Satoh M. Polymer 2002;43:103–10.
[38] Bard AJ, Faulkner LR. Electrochemical methods: fundamentals and apllications. Hoboken, NJ: Wiley; 1980.
[39] Huang WS, Humphrey BD, MacDiarmid AG. J Chem Soc, Faraday Trans I 1986;82:2385.
[40] Boudreaux DS, Chance RR, Wolf JF, Shacklette LW, Brédas JL, Thémans B, et al. J Chem Phys 1986;85:4584.
[41] Paul EW, Ricco AJ, Wrighton MS. J Phys Chem 1985;89:1441.
[42] Shacklette LW, Wolf JF, Gould S, Baughman RH. J Chem Phys 1988;88: 3955.
[43] McManus PM, Yang SC, Cushman RJ. J Chem Soc, Chem Commun 1985;1556.
[44] Kitani A, Kaya M, Sasaki K. J Electrochem Soc 1986;133:1069.
[45] Park YW, Lee YS, Park C, Shacklette LW, Baughman RH. Solid State Commun 1987;63:1063.
[46] Barsoukov E, Macdonald JR. Impedance spectroscopy: theory, experiment, and applications. Hoboken, NJ: Wiley; 2005.
[47] Vasik J, Kopecek J. J Appl Polym Sci 1975;19:3029.
[48] Pissis P, Kyritsis A. Solid State Ionics 1997;97:105.
[49] Matveeva ES, Diaz Calleja R, Parkhutik VP. Electrochim Acta 1996;41: 1351.
[50] Sulimenko T, Stejskal J, Krivka I, Prokes J. Eur Polym J 2001;37:319.
[51] Quadrat O, Stejskal J, Kratochvìl P, Klason C, McQueen D, Kubàt J, et al. Synth Met 1998;97:37.